J. Bangladesh Acad. Sci. 44(2); 161-178: December 2020 DOI: 10.3329/jbas.v44i2.51460

Journal of Bangladesh Academy of Sciences

Journal homepage: http://www.bas.org.bd/publications/jbas.html

Research Article

Numerical computation of natural ventilation system at the top floor of a multistory building in Dhaka city

Md. Zavid Iqbal Bangalee, M. Ferdows, Roushanara Begum[1]

Department of Applied Mathematics, University of Dhaka, Dhaka, Bangladesh

ARTICLE INFO

Article History

Received: 25 October 2020

Revised: 24 December 2020

Accepted: 28 December 2020

Keywords: k–ε turbulence model, Computational fluid dynamics, Natural ventilation, Thermal comfort.

ABSTRACT

Urban environment studies have become more and more critical in the past decades because of the rapid development of urbanization in industrial countries. Temperature, velocity, average mass flow, etc. at different unit an the top floor of a multistory building are discussed here. For the numerical computation of the air flow inside the building rooms, the k–ε turbulence model is used. ANSYS CFX software is usedto solve the governing equations. For modeling the building, Bangladesh, national building code is applied. The turbulence model is also validated by comparing the result with an experimental result and a numerical result. Satisfactory ventilation rate is also ensured by comparing the result with ANSI/ASHRAE Standard 62.1-2004.

Introduction

Cities are dynamic in nature. These develop because of interaction between different social, political, economic and technological forces. With the development of technology, taller and taller structures are being designed and constructed to care for the local need and desires.Such structures significantlyaffect the surrounding wind patterns due to the change in the local wind flows.

Many computational fluid dynamics (CFD) studies were performed to investigate the wind field characteristics within a building complex and around high-rise buildings at a pedestrian level.Adequate natural ventilation is achievable even in dense urban areas if building regulations are carefully devised and building configurations are carefully arranged. Maximum Allowable Building Footprint (MABF) of 70% provides higher ventilation rates, above 30 ACH (air change per hour) in maximum number of dwelling units (Islam, 2013).

Applying the CFD as an effective tool to simulate the urban wind flowing across the neighborhood, city planners can better understand a conceivable physical environment of the urban areas (Yang et al., 2013). CFD is a powerful tool for investigating building air flow applications and provides detailed predictions of air velocities around buildings (Varkute andMaurya, 2013;Mohamed et al., 2010). The gap between the two buildings is significant and needs to be investigated before planning, and anexcellent natural ventilated location around an existing one can be easily located with the help of CFD analysis.

*Corresponding author:<zavid@du.ac.bd>

[1]Department of Mathematics, American International University-Bangladesh, Bangladesh.

Three main approaches are commonly employed for studying natural ventilation: full-scale and wind tunnel experiments, and numerical modeling with computational fluid dynamics (CFD). The advantage of CFD is that it provides information on the flow field variables without the difficulty of CFD is that it provides information on the low field variables without the problem of controlling experimental conditions (like full-scale experiments) and without similarity constraints (Jiru et al., 2010). The contributions from analytical and empirical models are around 5%, where the CFD models account for 70% of the ventilation performance studies published in the past year (Qingyan, 2009).

In an apartment building located in a densely populated urban neighborhood, a built-in fan should control the air flow direction and avoid cross-contamination. The fan-assisted ventilation system approach provides thermal comfort in a temperature band somewhere above 20 °C and below 30 °C. This approach is much cheaper to operate than full air-conditioning (Liu et al., 2016). Except for the geometry of the openings of a building and the incidence angle of the wind, the magnitude of the wind velocity plays an important role in the air change rate of a building due to its proportionality to the inlet volume flow rate. In order to have uniform ventilation of the building, an in-depth study of its inner geometry is necessary (Nikas et al., 2014).

The use of solar chimney for natural ventilation of buildings is a widely used architectural technique known from Roman times. A multi-story solar chimney is an exciting option that could be applied to hot climates to save energy. (Fidaros, 2010; Punyasompum et al., 2009). The indoor environment affects human health directly. Different window-opening behavior results in a different indoor environment. Natural ventilation affects the distance between two openings and the location of openings (Nie et al., 2015).

In numerous European countries, residential ventilation standards specify minimum ventilation requirements in bedrooms, living rooms, or both. In the United States, ASHRAE Standard 62.2 (Ashrae, 2004), Ventilation and Acceptable Indoor Air Quality in Low-Rise Residential Buildings specify an acceptable minimum whole-house ventilation rate that depends on the timing of ventilation air delivery; however, it is silent about the distribution of ventilation air. The Washington State Ventilation and Indoor Air Quality Code (WAC 2004) are also quite about ventilation air distribution. Both the Minnesota Building Code (MN Chapter 7672) and the National Building Code of Canada (NBC 2005), which refer to Canadian Standard F326-M91 (CSA 2005), require whole-house ventilation air distribution via a fully ducted ventilation system or by mixing via a central air-handling system.

There is no standard condition found to date which is accepted as a satisfied condition by 100% of occupants due to the personal level differences (e.g., clothing, adaptation, body condition). The standards are proposed based on majority's sensation and feeling (Olesen, 2005). In most standards and guidelines for the indoor air quality is related to a required level of ventilation (ASHRAE 2004). The standard ventilation rate for an occupied space depends on the number of persons, floor area and smoking habit of those persons.

The flu like symptoms of the people living on that often disappear when people are away from the building are termed as sick building syndrome (SBS) in medical science. Problems associated with SBS are a common environmental health issue nowadays. In 1983, the World Health Organization (WHO) defined SBS as the symptom of eye, skin, nose, throat irritation, mental fatigue, headaches, nausea and dizziness. Furthermore, suffering from asthma is partly attributed to low indoor air quality due to the lack of proper ventilation (Olesen, 2005). It was also reported that an increased ventilation rate would increase the occupants' performance by 5 to 10%. Limiting the pollution sources, improving air quality by air cleaning, or increased ventilation rates may increase the performance, sleep quality, and even occupants' recreation level. It is evident that the ventilation system in the building is largely responsible for SBS (Morey and Shattuck, 1989). Therefore, a ventilation system performs a vital role in removing indoor pollutants and sick building syndrome.

Model Geometry

A lot area of 7200 ft^2 (10 Katha) is chosen for numerical simulation. An eight-storied building is considered enclosing 80% area (5760 ft^2) of total lot area to comply with the building code for Dhaka city. Though 70% maximum allowable building footprint (MABF) is the best option to be chosen, 80% MABF is chosen because it is the most common building type in Bangladesh [2013]. Each of the floors has four units (Fig. 4) of equal area (1400 ft^2). The area (Length × Width) of each unit is 38 ft × 35 ft (11.585 m × 10.67 m). The height of the entire building is 6.592 ft (26.4 m). The remaining 160 ft^2 (14.872 m^2) is kept for the staircase.

Each of the units has three living rooms, two bathrooms and a kitchen room (Fig. 1b). Each floor's dimension and ceiling height are chosen following the Bangladesh National Building Code-2012 [2012]. The dimension of the opening positions in each room is also kept following this code. The thickness of the outer walls and the ceilings are kept to be 0.5 m, and the thickness of the inner partitions between any two rooms are kept to be 0.3 m. The height of each floor is 2.8 m (without ceiling thickness). The dimension of each of the living rooms is 4.698 m × 4.698 m (15 ft × 15 ft). The dimension of the kitchen room is 3.659 m × 3.049 m (12 ft × 10 ft) and each of the bath rooms is 3.049 m × 2.439 m (10 ft × 8ft). The remaining floor area may be used as the dining space.

The dimension of the exit door is 3.5 ft × 7 ft (width × height). The dimension of each of the doors of living rooms is kept the same as the exit door. The dimension of the kitchen and bath room doors is kept as 3 ft × 7 ft (width × height). Six windows are kept in each unit (one in living room-1, two in living room-2, and one at each bath and kitchen room). Each of the windows of living rooms is 6ft × 4.5 ft (width × height) at the height of 0.762 m from the floor. The window of the kitchen room is 4.5 ft × 3.5 ft (width × height) at the height of 1.22 m from the floor and the window of the bath room is 3.5 ft × 1.64 ft (width × height) at the

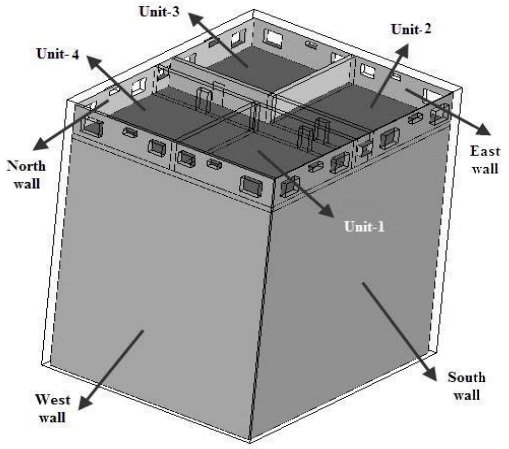

Fig. 1(a). Unit distribution on the top floor without room partitions.

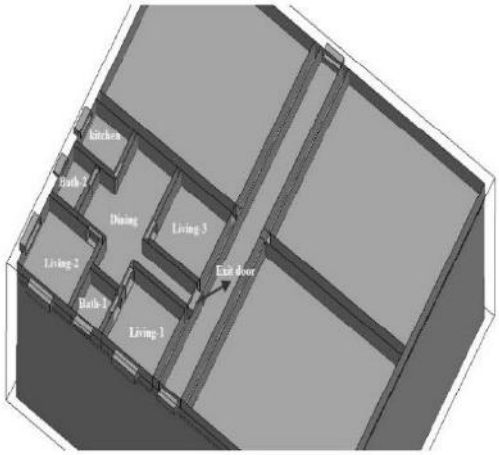

Fig. 1(b). Room partitions, doors, and windows in unit-1.

height of 1.995 m from the floor. Two windows are kept at the staircase area (one at the south wall and the other at the north), each of 4.5 ft $\times$ 3 ft (width $\times$ height) at the height of 1.22 m from the floor.

An extended computational domain is assumed around the building to observe the flow phenomena outside the building. An extended boundary is assumed at 3.6 H m far from the south (front) wall, 10H m far from the north (rear) wall, 6H m far from the top wall, and 5H m far from both the east and west (lateral) walls. Only the eighth floor (top floor) is shown in the figure.

Fig.1a and Fig.1b show four units on the eighth floor and room distribution in unit-1, respectively. All four units on each floor are of identical physical geometry.

Grid Analysis

All the units on each floor are identical. For this reason, simulations are performed only in one of the units (unit-1). Grid analysis performed by considering all the windows of unit-1 and doors inside it as open and all other windows and doors of other units as closed. So, fluid only enters unit-1 through the windows. The unstructured mesh is generated for numerical simulation. Fig. 2a shows the mesh distribution on a cut plane and surface mesh on the building and unit-1. The denser mesh is used close to the windows and the boundary walls (Fig. 2b).

Maximum element of the Global mesh size of Grid-4 is chosen as 7500 with scale factor 1. The part mesh is also used. The maximum element size at the inner layer of the building boundary and at the window frames is set as 200. At the outer layer of the building boundary maximum element size is 450 and at the extended computational domain boundary, it is 4000.

Five different grids have been generated. Among these, Grid-4 with 2544904 tetrahedron elements has been chosen for further simulations. The difference in mass flow average velocity through one of the windows opening with Grid-4 is presented in Table 1. It is observed from the table that the difference with Grid-4 in mass flow average velocity has negligible effects on the grid. If we increase the total number of elements, the change in average velocity is negligible (2.75%).

Table 1. Difference in mass flow average velocity in an opening position.

Grid (No. of elements)	Grid-1 (454911)	Grid-2 (995884)	Grid-3 (1653880)	Grid-4 (2544904)	Grid-5 (3539246)
Converged residual	10^{-3}	10^{-4}	10^{-5}	10^{-4}	10^{-3}
Mass flow average velocity [m/s]	0.66866	0.672356	0.76309	0.802504	0.824591
Difference with Grid-4	-16.68%	-16.22%	-4.9%	-	2.75%

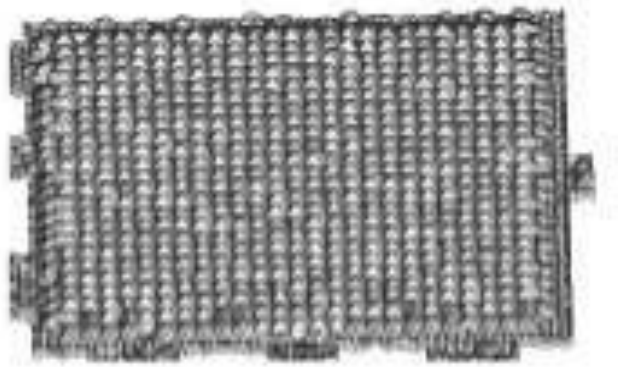

Fig. 2(a). Volume mesh on a cut plane through unit-1.

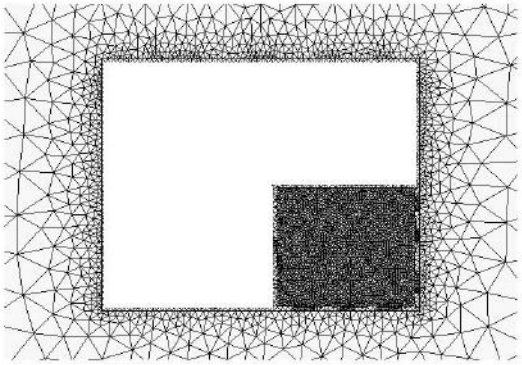

Fig. 2(b). Surface mesh on the building and denser mesh close to the building boundary.

Methodology

Nomenclature

u, v, w X, Y, Z-components of velocity respectively [ms^{-1}]

x, y, z Cartesian coordinates [m]

β Thermal expansion coefficient [K^{-1}]

μ Dynamic viscosity [Kg $m^{-1}s^{-1}$]

μ_T Turbulence viscosity [Kg $m^{-1}s^{-1}$]

ν Kinematic viscosity [m^2s^{-1}]

C_p Specific heat capacity [J $Kg^{-1}K^{-1}$]

T* $(T-T_C)/\Delta T$

ρ Density of the fluid [Kg m^3]

σ_T Thermal diffusivity [m^2s^{-1}]

L Length [m]

W Width [m]

H Height [m]

P Pressure [Kg $m^{-1}s^{-2}$]

k Turbulent kinetic energy [m^2s^{-1}]

g Gravitational acceleration [ms^{-2}]

ε Dissipation rate

Pr Prandtl Number

Governing equations and boundary conditions

CFD is based on the resolution of the governing equations which describe the flow field in the computational domain, namely the continuity equation for mass transfer, the N avier-Stokes equation for momentum transfer and the thermal energy equation for heat transfer. These equations for this problem can be written as follows:

Continuity equation:

$$\frac{\partial}{\partial x_j}(u_j) = 0; \quad j = 1, 2, 3; \qquad (3.1)$$

Momentum equation:

$$\rho u_j \frac{\partial}{\partial x_j}(u_i) = -\frac{\partial p}{\partial x_i} + \frac{\partial}{\partial x_j}[(\mu + \mu_T)\frac{\partial u_i}{\partial x_j}] +$$

$$\rho_{ref} g_i \beta (T - T_{ref}); \; i = 1, 2, 3; \; j = 1, 2, 3; \quad (3.2)$$

Energy equation:

$$u_j \frac{\partial}{\partial x_j}(T) = \frac{\partial}{\partial x_j}[(\frac{\nu}{\Pr} + \frac{\nu_T}{\sigma_T})\frac{\partial T}{\partial x_j}];$$

$$j = 1, 2, 3; \quad (3.3)$$

ding to the $k - \varepsilon$ model, μ_T can be expressed as follows:

$$\mu_T = C_\mu \rho \frac{k^2}{\varepsilon} \qquad (3.4)$$

and ε can be obtained from the following equations:

$$\frac{\partial}{\partial x_j}(\rho u_j k) = \frac{\partial}{\partial x_j}[(\mu + \frac{\mu_T}{\sigma_k})\frac{\partial k}{\partial x_j}] + P_k - \rho\varepsilon;$$

$$j = 1, 2, 3; \quad (3.5)$$

$$\frac{\partial}{\partial x_j}(\rho u_j \varepsilon) = \frac{\partial}{\partial x_j}[(\mu + \frac{\mu_T}{\sigma_\varepsilon})\frac{\partial \varepsilon}{\partial x}] + C_1 \frac{\varepsilon}{k} P_k -$$

$$C_2 \rho \frac{\varepsilon^2}{k}; \; j = 1, 2, 3; \quad (3.6)$$

Here P_k is the production rate of turbulent kinetic energy, which depends on the turbulent viscosity and velocity distribution. The values of all the empirical constants used in previous equations are presented in Table 2.

Table 2. Empirical constants used in $k - \varepsilon$ model.

C_μ	0.09
C_1	1.44
C_2	1.92
σ_k	1.0
σ_ε	1.3

Boundary Conditions

The following boundary conditions and locations are used at 25^{0}C isothermal temperature:

i. Opening at zero relative pressure: North wall of the computational domain
ii. No-slip wall with 0.28 mm roughness: Ground of the computational domain
iii. Symmetry wall: Top, east and west walls of the computational domain
iv. No-slip wall with 0 mm roughness: Building outer layers
v. No-slip and smooth wall: Building inner layers, door and window frames
vi. Inlet boundary conditions: Following inlet boundary conditions are used at the south wall of the computational domain:

Normal speed,

$$U(z) = \frac{u^*}{k} \ln(\frac{z + z_0}{z_0})$$

$$u^* = \frac{0.42 U_{ref}}{\ln((H + z_0)/z_0)}$$

$$I(z) = \frac{1}{\ln(z / z_o)}$$

$$k(z) = (I(z) * U(z))^2$$

$$\varepsilon(z) = \frac{u^{*3}}{0.42(z + z_o)}$$

where U_{ref} = 1.28 m/s, which is the average wind speed at Dhaka during the month of October (Bangladesh metereological department), when this simulation was being done.

Z_0 = 0.000025 m,

H=26.4 m, which is the total height of the building.

The inlet velocity increases with the increase in height.

Model Validation

Cross ventilation and single-sided ventilation, these two are the common ventilation patterns in the wind-driven natural ventilation system. In a single-sided ventilation system, the openings are located on one side of the building, and in the cross-ventilation system, two or more openings are present on opposite sides of the building. Jiang et al. (2003) reported the experimental result for both the single sided (opening on windward and leeward wall) and cross ventilation. Comparisons with Jiang et al. (2003) and Evola et al. (2006) are presented here to validate the numerical method used in this study.

Comparison with the results reported by Jiang et al. (2003)

Single sided ventilation through an opening located in the windward wall is simulated here, and the result is compared with the experimental result reported by Jiang et al. (2003). The result is also compared with the numerical result reported by Evola et al. (2006) for this model. A building like a cube with dimension 250 mm ×250 mm × 250 mm (length × height× width) and a door like opening with dimension 84 mm × 125 mm (length × height) on the windward wall of this cube is assumed here. The thickness of the walls is 6 mm. An extended computational domain, same as used by Jiang et al. is chosen. A downstream length of 8 H, an upstream length of 4 H, a lateral length of 4 H on both sides of the building and a height of 4 H are used as a computational domain where H = 250 mm is assumed as the reference length. Fig. 4 shows a schematic view of the building model with an opening in the windward wall.

The velocity profiles were measured by Jiang et al. (2003) at 18 measuring points along 10 vertical lines. Fig. 5 shows the locations of these measuring lines. ANSYS CFX [40] software is used to simulate the problem in this study. The problem has been simulated by using the $RNG\, k-\varepsilon$ model and $k-\varepsilon$ model.

A non-uniform structured mesh is used in both the cube and extended computational domain. 101×62 × 78 grids with about 0.49 million elements in the building like cube and 138×78×138 grids with about 1.4 million elements in the extended computational domain with stretching factor 1.1 and 1mm initial height are used. The denser mesh is used in the building around the opening and just outside the building to capture the flow phenomena accurately. The grid distribution on the building and the extended computational domain is shown in Fig. 6.

At the inlet boundary a normal speed as following is applied:

$$U\,(h) = \frac{U_o}{k}.1\,n\,(\frac{h}{h_o})$$

where h is the distance from the ground, k = 0.41 is the Von Karman's constant, U_0=1.068 ms^{-1}, and h_0=0.005 m. The velocity components along vertical and spanwise directions are assumed to be zero. The following relations are also used for k and ε in the inlet boundary:

$$k = \frac{3}{2}(U_{avg}.T_i)^2 \text{ and } \varepsilon = C_\mu^{3/4}\frac{k^{3/2}}{l_t}$$

where U_{avg} is the average flow velocity, T_i=4% is the turbulence intensity and l_t=0.4 m is the turbulence length scale. All the above parameters are used as Evola et al. (2006), which had been determined through the best fit of the experimental data provided by Jiang et al. (2003). At the outlet opening of the computational domain, zero relative pressure and zero gradients are used.

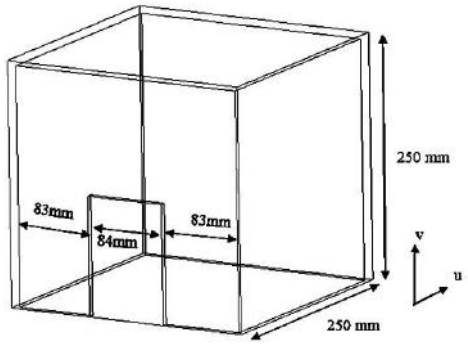

Fig. 4. Schematic view of the model (Single sided ventilation in the windward wall).

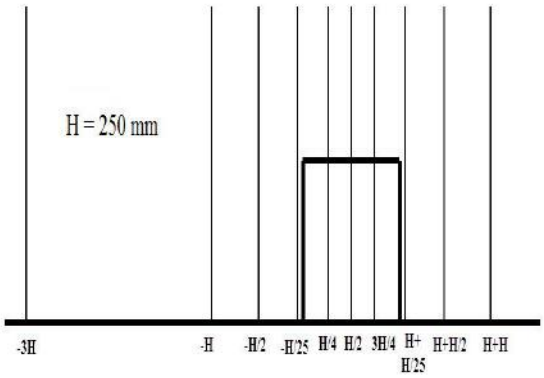

Fig. 5. The locations of the lines along which the velocities are measured.

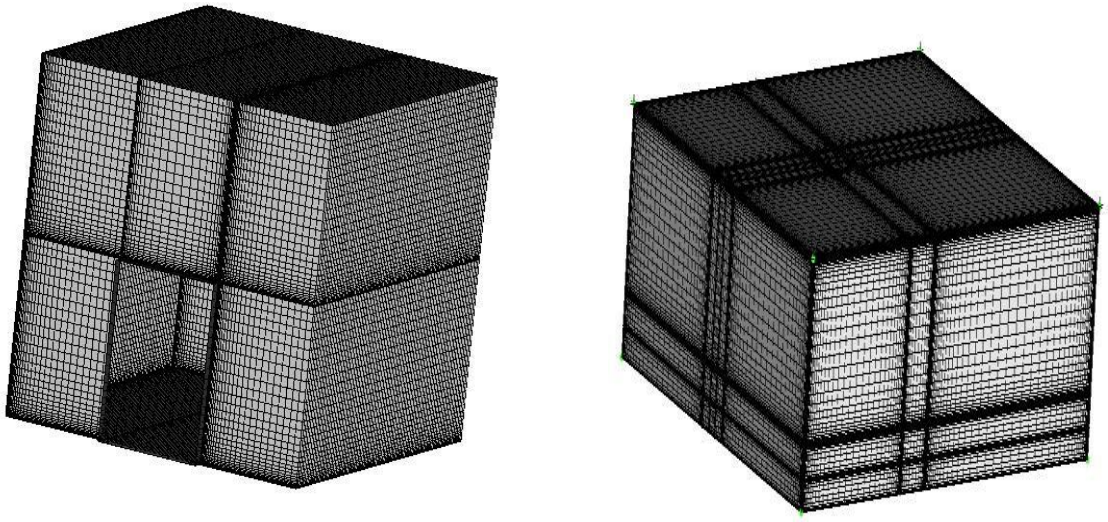

Fig. 6. Grid distribution in the (left): building like a cube (right): Extended computational. domain.

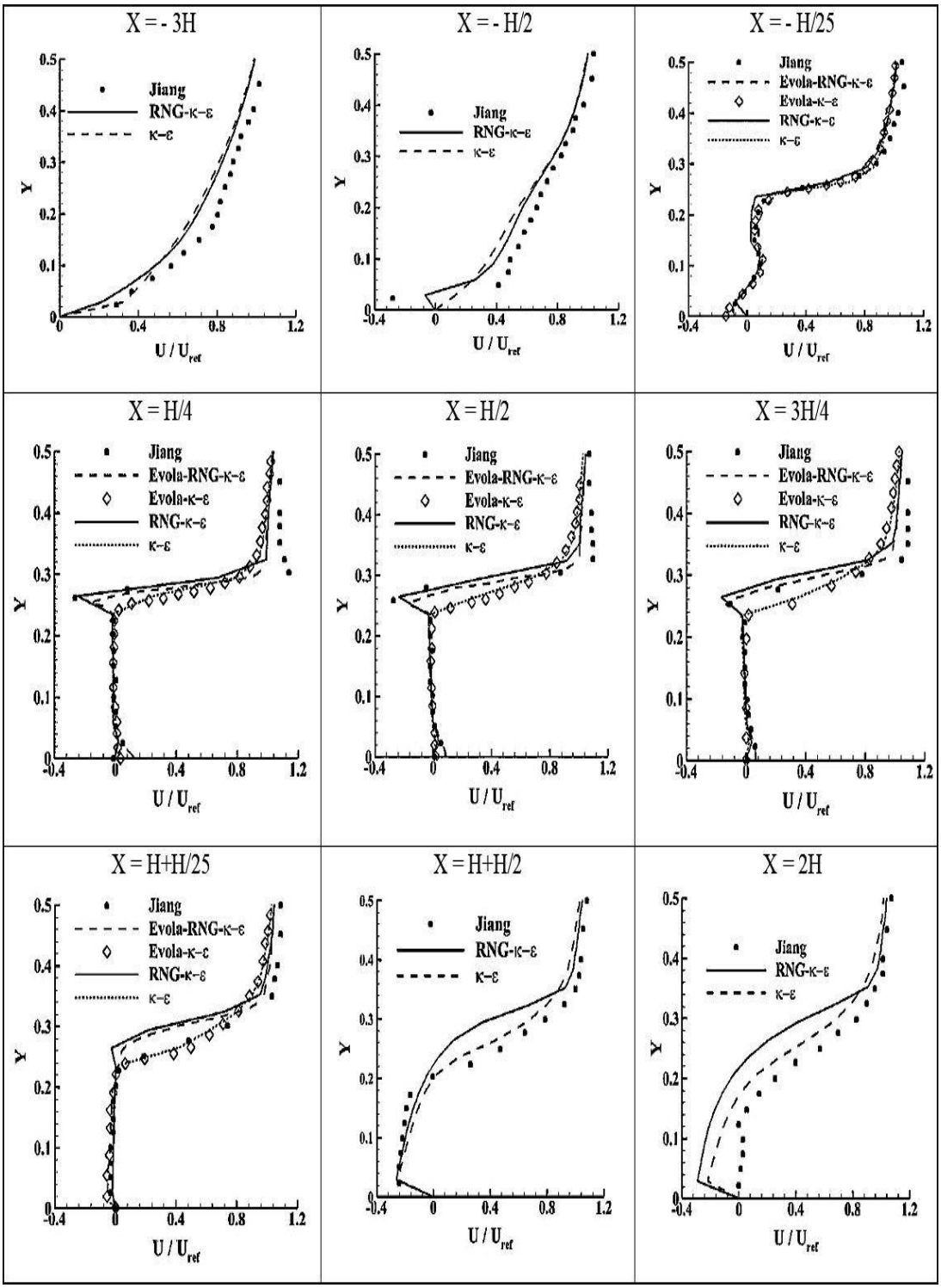

Fig.7. U-velocity distribution for single-sided windward ventilation.

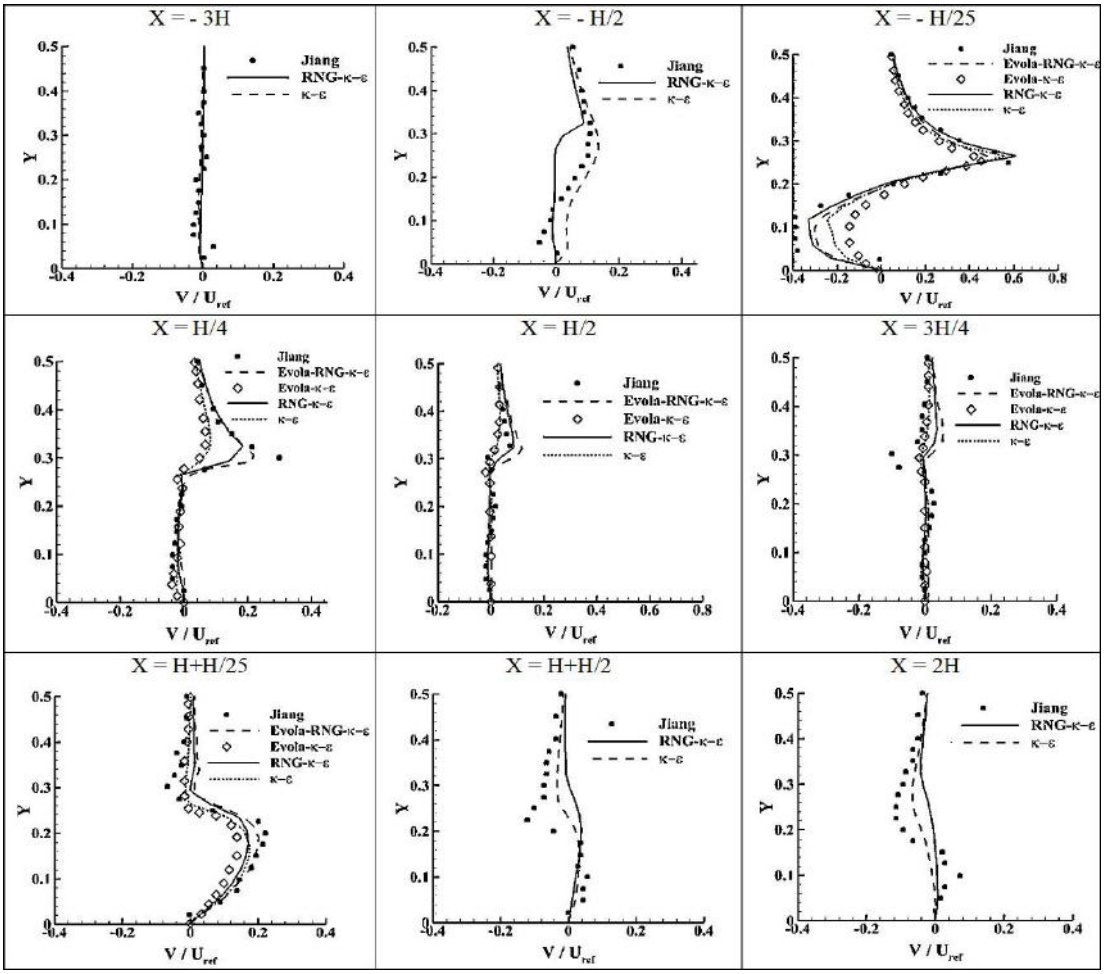

Fig. 8. V-velocity distribution for single sided windward ventilation.

Figure 7 and 8 show the comparison of the U-velocity and V-velocity profiles respectively for these two models with the experimental result of Jiang et al. (2003) and the numerical results of Evola et al. (2006).

The U and V velocities are normalized dividing by the reference velocity U_{ref} =12 ms^{-1} which is the maximum stream wise velocity measured in the experimental tests. Good agreement is observed between the experimental and numerical results inside the building and close to the opening which is the main purpose in natural ventilation design.

Some discrepancy is observed over the building roof and outside the building and more discrepancy is found behind the building which is in full agreement with the other studies which illustrates the inaccuracy of RANS models in the separation region above and behind the building. Comparing the results with the experimental results it is clear that, the present result using $RNG\,k-\varepsilon$ model gives better performance than $k-\varepsilon$ model and even better than the results reported by Evola et al. (2006).

Results and Discussion

On each floor, there are four units which are physically identical (all kinds of dimensions). But the average mass flow and velocity may change because of the position of these units with respect to the inlet and outlet position and other boundary conditions in the extended computational domain. For the convenience of the discussion, planes through the six windows in each unit are numbered as plane-1, plane-2, etc., as shown in Fig. 9.

Comparison and mass flow analysis in unit-1 of eighth floor

In this section, two simulations are done, and their results are compared. First simulation is done as an only unit-1 of eighth floor (height = 23.1 m to 25.9 m) to be open and another one is all the units of this floor to be open. In both of this cases, south wall is considered as an inlet and north wall as outlet. Table-3 shows average mass flow through different windows of unit-1 of eighth floor, keeping unit-1 open and then

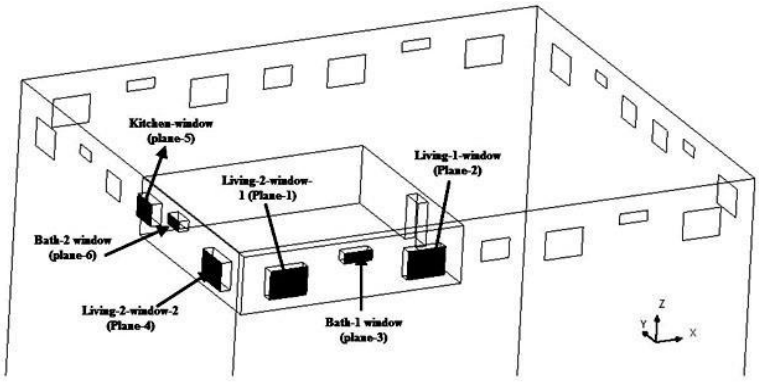

Fig. 9. Unit-1 with all windows and corresponding plane no.

Table 3. Average mass flow through different windows of unit-1 for two different cases.

Position	Area (m^2)	Density (Kg/m^3)	Average velocity (Unit-1-open) (m/s)	Mass flow (Kg/s)	Average velocity (All unit-open) (m/s)	Mass flow (Kg/s)	Error (%)
Plane-1	0.02511	1.185	0.593413	0.01766	0.598346	0.0178	0.83129
Plane-2	0.02511	1.185	0.578573	0.01721	0.578638	0.01722	0.01123
Plane-3	0.00686	1.185	0.402128	0.00327	0.404299	0.00329	0.53988
Plane-4	0.02511	1.185	0.553110	0.01646	0.571945	0.01702	3.40529
Plane-5	0.01464	1.185	0.488540	0.00847	0.499006	0.00866	2.1423
Plane-6	0.00534	1.185	0.418072	0.00264	0.430259	0.00272	2.91505

all units open. Error in average mass flow through each window for these two cases is also reported here. It is observed that maximum error is 3.40%, which is negligible. Velocity profiles at the mid height of unit-1, through mid-width and length respectively are shown in Fig. 10(a) and 10(b). Velocity profiles for both cases are also similar. Higher velocity is observed at south wall windows than west wall windows because of the inlet position which was in south wall.

Fig. 11 shows velocity vectors through all the windows of unit-1 for both cases. It is observed that south wall windows always behave as inlet and west wall windows as an outlet. So, by keeping all windows open, maximum thermal comfort may be assured.

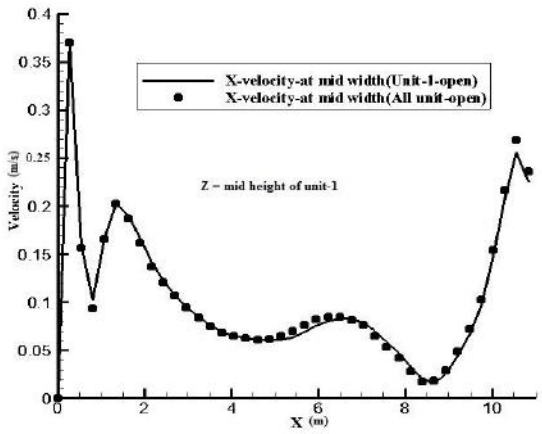

Fig. 10(a). Velocity profiles at mid-width of unit-1.

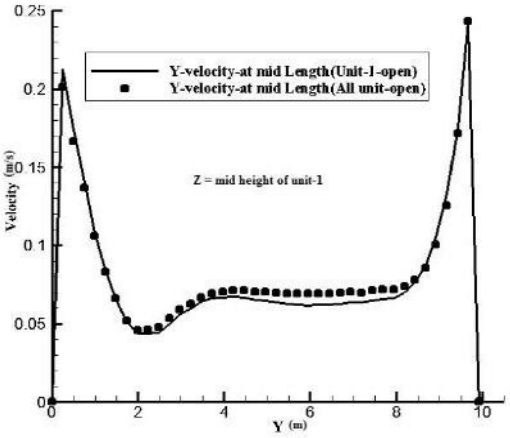

Fig.10 (b). Velocity profiles at mid length of unit-1.

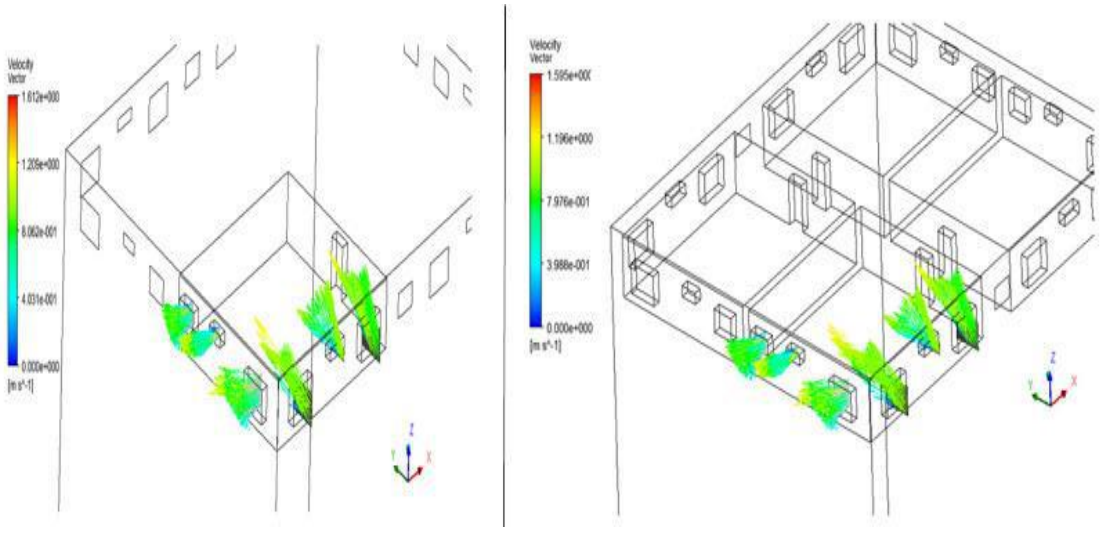

Fig. 11. Velocity vector through different windows of unit-1 (only unit-1 open (left) and all units open (right).

Figure 12 shows the velocity profiles at three different positions of three windows (two in south wall and one in west wall) for both cases which shows that air flow velocity change is negligible at different height of each windows. Lower velocity is observed adjacent to the window frame than mid position of a window which is because of the disruption of air by the surface. So, it can be said that for negligible height difference air flow does not change a lot and air will enter through a window at a same rate. Similar behavior is observed for other windows also.

Finally, Fig. 13 and 14 show velocity contours at different planes through each window. These velocity profiles and contours show similarity in both cases. It is also observed from the velocity contours that flow velocity is higher around the mid position and bottom right corner of the windows located on south wall. Similarly, this velocity is higher around the mid position and upper part of the windows located in west wall.

It can be concluded from avobe discussion that, every unit is independent in flow pattern and has no effect in ventilation rate of other units. Air will pass through the windows which are present in that unit only.

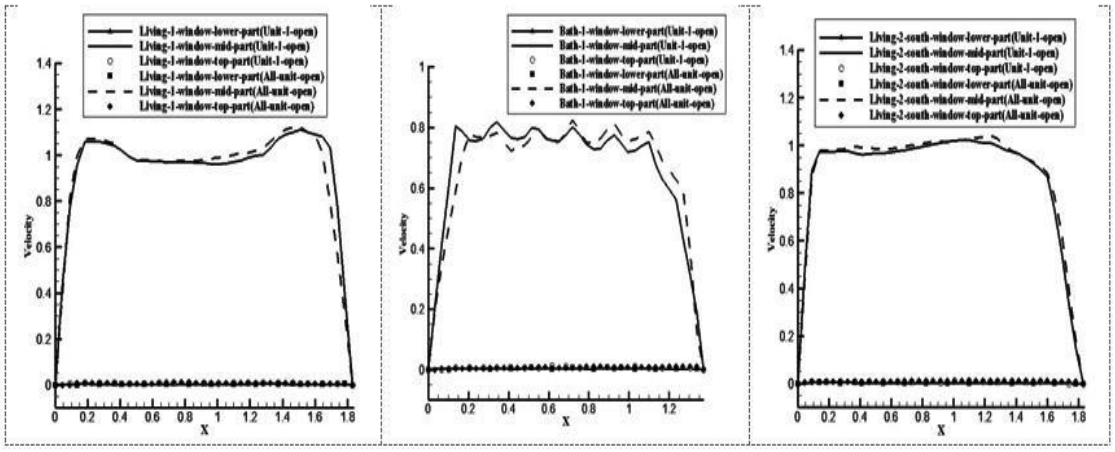

Fig. 12. Velocity profiles at different height of windows of unit-1 for both cases.

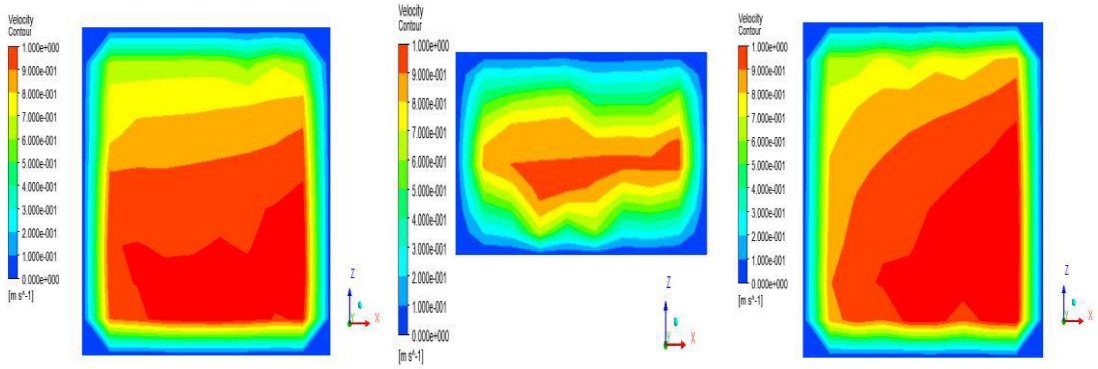

Plane-1 (Living-2-south-window) **Plane-3 (Bath-1-window)** **Plane-2 (Living-1-window)**

Fig. 13(a). Velocity contours at different windows of unit-1, keeping unit-1open (South-wall windows).

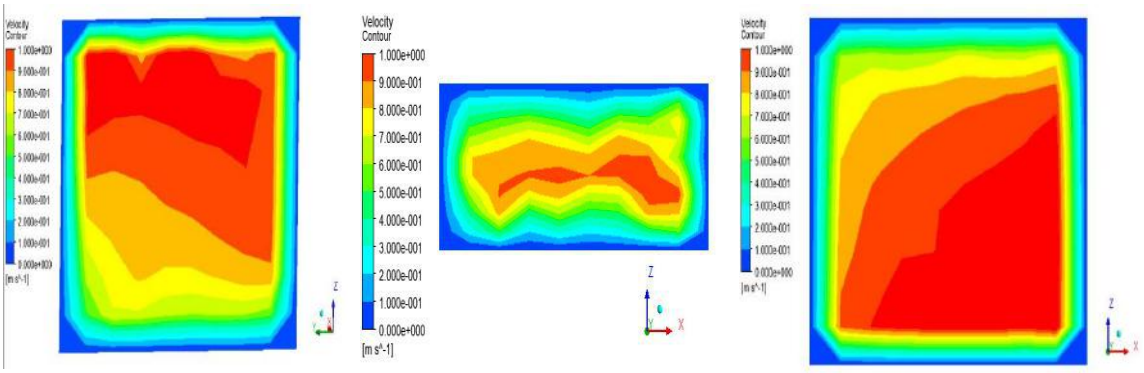

Plane-1 (Living-2-south-window). Plane-3 (Bath-1-window). Plane-2 (Living-1-window).

Fig. 13(b). Velocity contours at different windows of unit-1, keeping all windows open (South-wall windows).

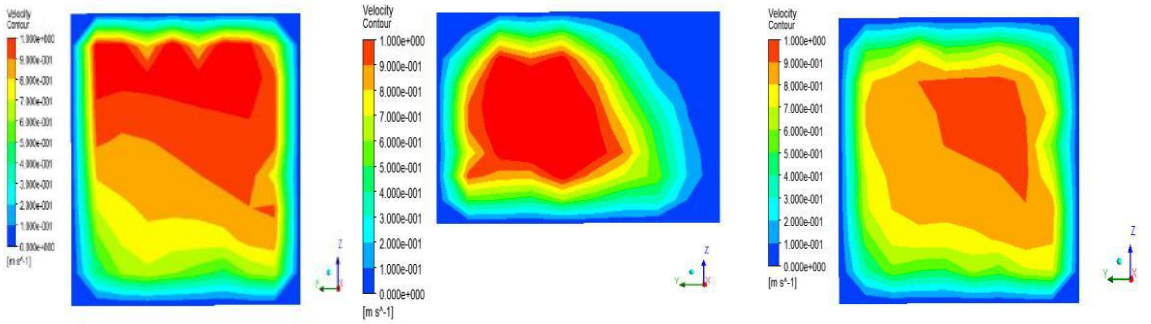

Plane-4 (Living-2-west-window) Plane-6 (Bath-2-window) Plane-5 (kitchen-window)

Fig. 14(a). Velocity contours at different windows of unit-1, keeping unit-1 open (west-wall windows).

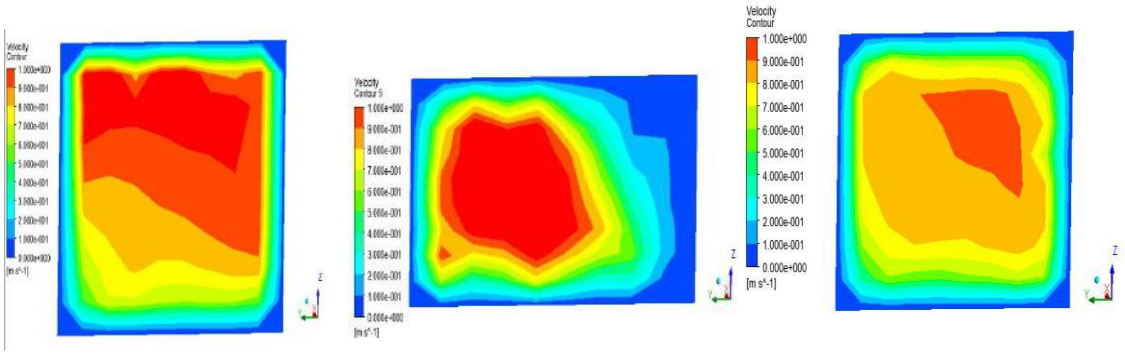

Plane-4 (Living-2-west-window) Plane-6 (Bath-2-window) Plane-5 (kitchen-window)

Fig. 14(b). Velocity contours at different windows of unit-1, keeping all windows open (west-wall windows).

Comparison and flow analysis in unit-2 and unit-4 of eighth floor

In this study, an eight storied building consists of four units on each floor is considered. Among these units, unit-1, and unit-2 are on the front side (south) and unit-3 and unit-4 are on the rear side (north) of the building. The South wall is considered as an inlet and the North wall as an outlet.

Table 4 shows average mass flow through different windows of unit-2 and unit-4. Comparing the mass flow data with Table 3, it is observed that difference in mass flow between unit-1 and unit-2 is negligible as expected. It is because this two units are both on front (south) side of the building. On the other hand, this difference is higher between unit-1 and unit-4 (which is on back / north side) since these are on opposite side of the building. Same behavior is also observed in velocity vectors and velocity contours through different windows of unit-2 and unit-4 which are represented in Fig. 15 to Fig. 18. The flow characteristics of unit-1 and unit-2 are almost identical. South wall windows behaving as inlet (air is entering through these windows) and east wall windows behaving as outlet (air is leaving through these windows).

But in unit-4, air is entering through the north wall windows and existing through west windows though north wall (Fig. 16) is considered as outlet (opening). Air is also entering in small amount through the west wall windows. It may occur because of the pressure difference as well as density difference in the rear side of the building.

Table 4. Average mass flow through different windows of unit-2 and unit-4 window).

Position	Area (m^2)	Density (Kg/m^3)	Average velocity (unit-2) (m/s)	Mass flow (Kg/s)	Error with unit-1 (Unit-1 open) (%)	Average velocity (unit-4) (m/s)	Mass flow (Kg/s)
Plane-1	0.02511	1.185	0.57479	0.01710	3.93769	0.173711	0.00517
Plane-2	0.02511	1.185	0.59409	0.01768	2.66972	0.184550	0.00549
Plane-3	0.00686	1.185	0.39357	0.00320	2.65398	0.145864	0.00119
Plane-4	0.02511	1.185	0.56432	0.01679	1.33369	0.091216	0.00271
Plane-5	0.01464	1.185	0.49010	0.00850	1.78455	0.227640	0.00395
Plane-6	0.00534	1.185	0.42744	0.00270	0.65472	0.133965	0.00085

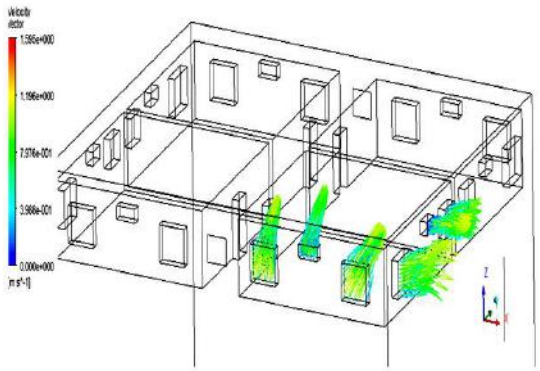

Fig. 15. Velocity vectors through different windows of eighth floor (Unit-2).

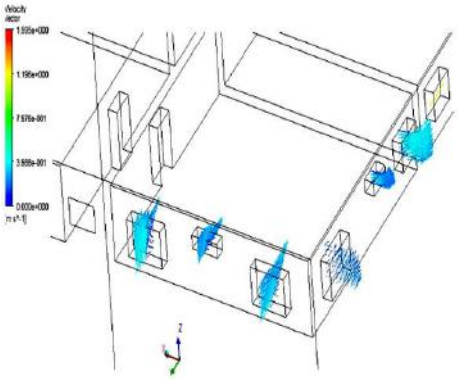

Fig. 16. Velocity vectors through different windows of eighth floor (Unit-4).

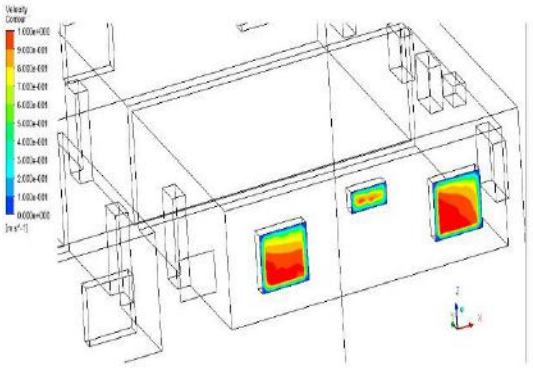

Fig. 17(a). Velocity contours on south wall windows of eighth floor (Unit-2).

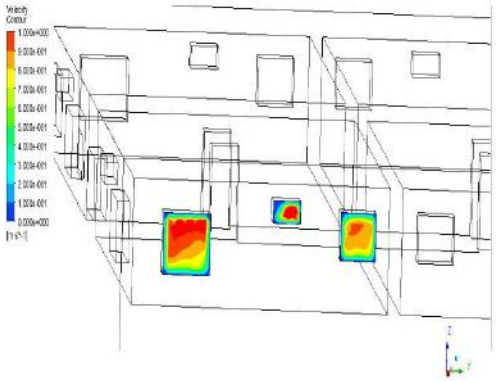

Fig. 17(b). Velocity contours on east wall windows of eighth floor (Unit-2).

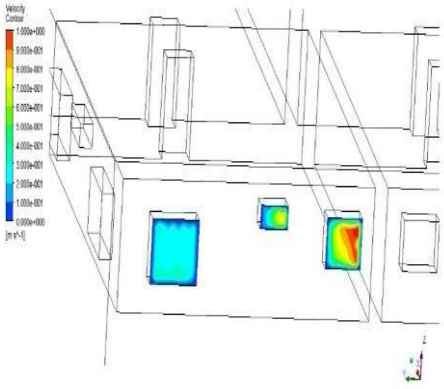

Fig. 18(a). Velocity contours on west wall windows of eighth floor (Unit-4).

Fig. 18(b). Velocity contours on north wall windows of eighth floor (Unit-4).

Ventilation Rate

The standard ventilation rate for an occupied space depends on the number of persons, floor area and smoking habit of those persons. The required ventilation rate for each person (smoker/non-smoker) was proposed by CEN-CR1752. It is observed that in this studied building ventilation rate is satisfactory. The observed rate is 38.3, which is enough for 6-8 persons in each unit.

Table 5. The required ventilation rate for each person (CEN-CR1752).

Standard	Class	Ventilation rate [gm/s]			
		Non-smoker	20% smoker	40% smoker	100% smoker
CR 1752	A	11.9	23.7	35.6	35.6
	B	8.3	16.6	24.9	24.9
	C	4.7	9.5	14.2	14.2

That means, Natural ventilation in this building plays a key role in providing optimum quality of indoor circulation of air within the building and maintaining acceptable level of thermal comfort without necessity for employment of mechanical systems such as Heating, Ventilation, and Air Conditioning (HVAC). The natural resources are abundant and free. If the mechanical ventilation system is replaced with a natural ventilation system, it may save a lot of energy. The green energy (e.g., wind and solar) provides the driving mechanism in this ventilation system. Natural ventilation system in this building may assist to save the electricity consumption.

Conclusion

An eight-storied building on a lot area of 7200 ft^2 (10 Katha) is chosen for numerical simulation enclosing 80% area (5760 ft^2) of total lot area to comply with the building code for Dhaka city. Each of the floors has four units of equal area (1400 ft^2). Simulations are done for different units of eighth floor.

It is observed that at the same height of a building the flow phenomena remain almost same in all units. Air change per hour (ACH) is also found to be satisfactory in this building. So, by following the national building code and MABF of 80% expected ventilation rate can be assured without any mechanical support.

Further study is necessary to observe the flow analysis at different floor of a building. Though the velocity increases with the increase of height, ventilation rate may be also assured in all other floors also.

Acknowledgement

Project under special allocation for Science and Technology 2014-2015, Ministry of Science and Technology, Bangladesh. Computational facilities available in the Department of Applied Mathematics, University of Dhaka, Dhaka 1000, Bangladesh.

References

ANSYS 12.0, Ansys Inc., User manual.

Evola G and Popov V. Computational analysis of wind driven natural ventilation in buildings. *Energy Build*. 2006; 38: 491–501.

Fidaros D. Numerical study of the natural ventilation in a dwelling with a solar chimney. *Passive and Low Energy Cooling for the Built Environment-PALENC-2010*;

29 September-1 October, 2010; Rhodes Island, Greece.

Islam S. A study on zoning regulations' impact on ventilation rate' in non-conditioned apartment buildings in Dhaka city. *Proceedings of the Solar Conference, World Renewable Energy Forum, American Solar Energy Society*, 2012; vol. 5: 3584-3591.

Islam S. An Extended Study on Building Regulations 'Impact on Natural Ventilation in Apartment Buildings in Dhaka City, CAA Dhaka, *20th General Assembly and Conference*, 2013.

Islam S. Impacts of 'Maximum Allowable Building Footprint' on Natural Ventilation in Apartment Building, *PLEA 2013 - 29th Conference, Sustainable Architecture for a Renewable Future*, 2013; September, p 10-12, Munich, Germany.

Jiang Yi, Donald A, Huw J, Rob A and Qingyan C. Natural ventilation in buildings: measurement in a wind tunnel and numerical simulation with large-eddy simulation. *J. Wind. Eng. Ind*. 2003; 91: 331–353.

Jiru TE and Bitsuamlak GT. Advances in applications of CFD to natural ventilation, *The Fifth International Symposium on Computational Wind Engineering (CWE 2010)*, May 23-27, 2010; Chapel Hill, North Carolina, USA.

Karava P, Stathopoulos T and Athienitis AK. Airflow assessment in cross-ventilated buildings with operable façade elements. *Build Environ.* 2011; 46: 266-279.

Liu Y and Moser A. Numerical study of hybrid ventilation of apartments in a densely populated urban neighborhood. *Int. J. Vent.* 2016; 1(3): 219-224.

Mohamed MF, King S, Behnia M, Prasad D and Ling J. Wind-driven natural ventilation study for multi-stored residential building using CFD, *44th Annual Conference of the Architectural Science Association*, 2010; ANZAScA, Unitec Institute of Technology.

Nie P, Zhou J, Tong B, Zhang Q and Zhang G. Numerical study on the effect of natural ventilation and optimal orientation of residential buildings in Changsha, China. *Procedia Eng.* 2015; 121: 1230-1237.

Nikas K-S, Nikolopoulos N, Nikolopoulos A. Numerical study of a naturally cross-ventilated building, *Energy Build.* 2010; 42: 422-434.

Olesen BW. Indoor environment-health-comfort and productivity, *Proceedings of Clima, 8th REHVA World Congress*, 2005; Lausanne, Switzerland. 1-17.

Punyasompun S, Hirunlabh J, Khedar J and Zeghmati B. Investigation of the application of solar chimney for multi-storey buildings. *Renew. Energy*, 2009; 34: 2545-2561.

Qingyan C. Ventilation performance prediction for buildings: A method overview and recent applications. *Build Environ.* 2009; 44(4), 848-858.

Ramponi R and Blocken B. CFD simulation of cross-ventilation for a generic isolated building: Impact of computational parameters. *Build. Environ.* 2012; 53: 34-48.

Varkute NS and Maurya RS. CFD simulation in township planning–A case study. *Int. J. Comput. Eng. Sci. (ijceronline.com)*, 2013; 3(3): 65-72.

Ventilation for Acceptable Indoor Air Quality, ANSI/ASHRAE Standard 62.1-2004.

Yang A-S, Wen C-Y, Wu Y-C, Juan Y-H, and Su Y-M. Wind field analysis for a high-rise residential building layout in Danhai, Taiwan. *Proceedings of the World Congress on Engineering*, July, 2013; Volume II: p 3-5.